ATMOSPHERIC ENVIRONMENT: X 12 (2021) 100122

Contents lists available at ScienceDirect

Atmospheric Environment: X

journal homepage: www.journals.elsevier.com/atmospheric-environment-x

Learning from the COVID-19 lockdown in berlin: Observations and modelling to support understanding policies to reduce NO_2.

Erika von Schneidemesser [a,*], Bheki Sibiya [a,b], Alexandre Caseiro [a], Tim Butler [a,b], Mark G. Lawrence [a,c], Joana Leitao [a], Aurelia Lupascu [a], Pedro Salvador [d]

[a] Institute for Advanced Sustainability Studies e.V., Berlinerstrasse 130, 14467, Potsdam, Germany
[b] Institut für Meteorologie, Freie Universität Berlin, Germany
[c] Institute of Environmental Science and Geography, University of Potsdam, Potsdam, Germany
[d] Department of Environment CIEMAT, Avda. Complutense 40, 28040, Madrid, Spain

ARTICLE INFO

Keywords:
Urban areas
Air pollution
Emissions
COVID-19
Nitrogen dioxide
Ozone
Europe

ABSTRACT

Urban air pollution is a substantial threat to human health. Traffic emissions remain a large contributor to air pollution in urban areas. The mobility restrictions put in place in response to the COVID-19 pandemic provided a large-scale real-world experiment that allows for the evaluation of changes in traffic emissions and the corresponding changes in air quality. Here we use observational data, as well as modelling, to analyse changes in nitrogen dioxide, ozone, and particulate matter resulting from the COVID-19 restrictions at the height of the lockdown period in Spring of 2020. Accounting for the influence of meteorology on air quality, we found that reduction of ca. 30–50 % in traffic counts, dominated by changes in passenger cars, corresponded to reductions in median observed nitrogen dioxide concentrations of ca. 40 % (traffic and urban background locations) and a ca. 22 % increase in ozone (urban background locations) during weekdays. Lesser reductions in nitrogen dioxide concentrations were observed at urban background stations at weekends, and no change in ozone was observed. The modelled reductions in median nitrogen dioxide at urban background locations were smaller than the observed reductions and the change was not significant. The model results showed no significant change in ozone on weekdays or weekends. The lack of a simulated weekday/weekend effect is consistent with previous work suggesting that NOx emissions from traffic could be significantly underestimated in European cities by models. These results indicate the potential for improvements in air quality due to policies for reducing traffic, along with the scale of reductions that would be needed to result in meaningful changes in air quality if a transition to sustainable mobility is to be seriously considered. They also confirm once more the highly relevant role of traffic for air quality in urban areas.

1. Introduction

Air pollution is the world's largest environmental risk for human health. A recent study with updated hazard ratio functions focused on the effects of outdoor air pollution (rather than both outdoor and indoor air pollution) attributed 8.9 million premature deaths to fine particulate matter (PM2.5; particles with an aerodynamic diameter of 2.5 μm or less) globally in 2015 (Burnett et al., 2018). This is substantially larger than the earlier estimate provided by the Global Burden of Disease study of 4.2 million premature deaths globally, also attributed to ambient PM2.5 in 2015 (Cohen et al., 2017). This suggests that outdoor air pollution is an even more important population health risk factor than previously thought (Burnett et al., 2018). Using the updated hazard ratio functions from Burnett et al. (2018), Lelieveld et al. (2019) attributed 790,000 premature deaths to air pollution annually in Europe. The World Health Organization (WHO) air quality guidelines are often exceeded in urban areas throughout Europe (EEA, 2020). Additionally, exceedances of the nitrogen dioxide (NO_2) limit values at traffic monitoring stations are a particular problem for many European countries owing mainly to the prevalence of diesel passenger cars, among other factors (EEA, 2019).

More recently, studies investigating the relationship between COVID-19 and air pollution have shown that areas with higher air pollution lead to greater COVID-19 mortality rates (Cole et al., 2020;

* Corresponding author.
E-mail address: evs@iass-potsdam.de (E. von Schneidemesser).

https://doi.org/10.1016/j.aeaoa.2021.100122
Received 27 May 2021; Received in revised form 16 July 2021; Accepted 25 July 2021
Available online 28 July 2021

Copat et al., 2020; López-Feldman et al., 2021; Pozzer et al., 2020; Travaglio et al., 2021). For example, Pozzer et al. (2020) showed that 15 % of COVID-19 mortality is attributable to anthropogenic air pollution worldwide. In Europe and Germany, 19 % and 26 % of COVID-19 mortality, respectively, was attributed to anthropogenic air pollution. These results have implications for policy and show that to foster sustainable cities that can build greater resilience for pandemics such as this one, clean air is a critical resource.

In response to the pandemic, many countries implemented different types of policy measures to limit the spread of the disease. These measures generally had a strong effect on mobility and specifically road transport emissions. From a scientific perspective, the COVID-19 'lockdown' policies provided a unique opportunity to evaluate substantial reductions in road transport and the subsequent effect on air quality as a large scale 'real-world experiment' that also reflects the potential of policies aimed at reducing road transport (Grange et al., 2020). The changes in road transport emissions allowed for an evaluation of what certain reductions in (mainly) passenger car traffic would change in terms of air quality, not only using observational data, but also modelling. And the changes in road transport emissions were substantial. As outlined by Guevara et al. (2020) an average at EU-30 level of 33 % reductions in NOx emissions was estimated. In addition, for NOx, NMVOCs, and PM2.5 more than 85 % of the total reduction in urban areas was attributable to road transport. However, there are confounding factors, such as meteorology and atmospheric chemistry that need to be accounted for to appropriately isolate the change attributed to the reduction in road transport (Kroll et al., 2020). While a slew of studies have been published that address changes in air quality during periods of 'lockdown' during the COVID-19 pandemic, some do not address the influence of these factors (e.g. Gama et al., 2021; Sicard et al., 2020b). Other studies that do consider, for example, the effect of meteorology, have shown that not accounting for these effects can substantially alter the amount of change in air pollution attributed to reductions in traffic emissions (Goldberg et al., 2020; Menut et al., 2020; Ordóñez et al., 2020).

In this paper we provide insights into (1) the potential for urban air quality improvements given reductions in transport emissions, and (2) the capacity of regional models to accurately predict changes in air quality based on emissions changes. In both cases, our overall aim is to leverage the potential from the COVID-19 lockdown measures in providing a real-world experiment to understand the effect of potential policies, and the dramatic change in emissions from passenger cars in urban areas on changes in air quality. To address these aims we have analysed air quality data from the city network of monitoring stations, in combination with traffic count data from five stations in Berlin. A classification of meteorological conditions was carried out to account for the influence of weather on air pollutant concentrations. Finally, an urban scale air quality model was run for Berlin using standard emissions and emissions adjusted to account for the decrease in traffic observed during the lockdown. These results were compared to the observational data to better understand how well the model performs predicting changes observed in the real world. The combination of these analyses is then used to provide a perspective on the capacity and limitations of models for projecting policy impacts, as well as assessing the scale of the policies that would be needed to adequately address NO_2 limit value exceedances that are a current problem for urban areas across Europe.

2. Methods

2.1. Berlin and lockdown

Berlin is the capital city of Germany with a slowly growing population of just over 3.7 million people (2019) in an area of 892 km^2 at a mean elevation of just 34 m above sea level. In 2018, 48.9 % of households in Berlin owned one or more passenger cars and 74.7 % owned one or more bicycles.[1] While Berlin has one of the lowest per capita car ownership rates for cities in the western world, it is still plagued by the usual issues in urban areas, including traffic jams, traffic accidents, and a large amount of urban space (58 % of Berlin's public street space (Creutzig et al., 2020)) devoted to car traffic and parking. The city also has multiple public transport options, including bus, tram, subway (S-Bahn), and underground (U-Bahn), in addition to being well connected on the regional European rail network, and internationally with two airports.

Throughout Germany, on average 57 % of trips are carried out with a car, 10 % with public transit, 11 % by bicycle, and 22 % by walking (data from 2017) (BMVI, 2018). If considered in terms of kilometres travelled, the amount travelled by car increases to 75 %, to 19 % for public transit, and only 3 % each for kilometres travelled by bicycle or walking nationally. However, the bigger the city, the fewer trips that are carried out by car and greater number carried out by public transport, bicycle, and walking, with car trips on average for metropolitan areas in Germany at 28 % (BMVI, 2018). In Berlin, by comparison, the modal split (from 2018/2019) is 26 % car, 27 % public transport, 18 % bicycle, and 30 % walking (Gerike et al., 2019).

In response to the COVID-19 pandemic, the city of Berlin (also its own federal state), started to shut down certain types of businesses, including gyms, clubs, bars, and cultural facilities on March 14, 2020. Three days later all schools and day cares were also closed. Exceptions were made for the children of parents with certain types of professions that were deemed 'essential,' such as nurses and doctors, people who worked in grocery stores, and similar. As of March 21, all restaurants and cafes were also closed, remaining open only for take-out. With the contact restrictions put into place on March 22, the period of full lockdown was begun. In Berlin, in contrast to many cities in Europe, people were still allowed to go outside for walks and recreation and did not need permits. However, any type of gathering in public places was not allowed, and more than two people were not allowed to meet, with the exception of families, households, or partners. This period of 'full lockdown' remained in place until April 20, at which point, some non-essential businesses were allowed to reopen, given that they had sufficient hygiene rules in place. A general overview of the timeline is given in Table 1.

2.2. Observations

In all cases, observational data were processed for 2016–2020, and subsequent analysis focused on differences in the core lockdown period between 22 March and 21 April for 2020 compared to 2016–2019.

2.2.1. Traffic

Hourly traffic counts for passenger vehicles and trucks[2] were obtained from the city of Berlin (Senate Department for Environment, Transport and Climate Protection) for five stations that correspond to the locations of five air quality monitoring stations classified as traffic stations (rather than urban background or rural). The location of the monitoring stations throughout the city can be viewed here: https://luftdaten.berlin.de/lqi. The data from the city covered all years from 2016 through the present. One station (Silbersteinstrasse) was omitted from the analysis, as construction activities in the direct vicinity of the station substantially altered the traffic patterns of the street starting in February 2020. The remaining four stations were analysed to understand the changes in traffic counts during 2020 and the COVID-19 restrictions relative to previous years. The changes in traffic counts were then used

[1] https://www.statistik-berlin-brandenburg.de/BasisZeitreiheGrafik/Bas-evs.asp?Ptyp=300&Sageb=63000&creg=BBB&anzwer=5.

[2] Traffic count data are provided as 'LKW' (German: Lastkraftwagen or English: truck) and 'PKW' (German: Personenkraftwagen or English: passenger car).

Table 1
Summary of lockdown phases in Berlin. Business as usual during pre-lockdown reflects the status quo prior to COVID-19, whereas the business as usual reflects a relatively open society after stricter measures have been lifted but still in the context of COVID-19. Any lockdown measures associated to the 'second wave' in the Fall of 2020 are not reflected.

Stage	Lockdown Type	Start date	End date	Days	Details of lockdown
1	Pre-lockdown	–	March 13, 2020	–	Business as usual
2	Partial lockdown	March 14, 2020	March 21, 2020	7	some businesses closed, some schools closed, more and more establishments close over time until the 22nd
3	Full lockdown	March 22, 2020	April 21, 2020	30	schools, daycares, parks, all non-essential businesses closed and people not allowed to gather beyond 2 people with members outside of family or household
4	Partial relaxation	April 22, 2020	June 21, 2020	60	contact restrictions still in place, but some smaller businesses allowed to open with hygiene measures
5	Full relaxation	June 22, 2020	–	–	Business 'as usual' (hygiene restrictions still in place for businesses, face mask requirements, etc.)

in the model runs to scale traffic emissions for the city for 2020.

To calculate the ratios, the traffic count data was first evaluated for anomalies, owing to possible construction or other events that would result in non-typical traffic count data. Two short-term anomalies were identified: (1) at the Mariendorfer Damm site passenger car traffic counts were much lower than normal, but truck traffic was not affected, between August 2016 and mid-February 2017, and (2) at the Frankfurter Allee site truck traffic counts had a substantial short-term spike at the beginning of 2016 through mid-February 2016, while car traffic counts were not affected. These time periods were removed so as not to skew the averages and ratios. In addition, changes to the traffic patterns on Karl-Marx-Strasse affected the traffic counts so that data from 2016 to 2018 represents the previous street design, while 2019 onward represents a different layout. For this reason, only 2019 data from Karl-Marx-Strasse was used to compare to 2020 values. Following the data cleaning, average values were calculated for each site for car traffic counts, truck traffic counts, and a total vehicle count, by month for Monday to Thursday (typical working days), Friday, Saturday, and Sunday to establish characteristic hourly traffic profiles by month and weekday. In this way, the emissions from traffic for the 2020 model run that reflected COVID-19 reductions were reduced based on changes in observed hourly traffic counts. The average traffic counts were calculated by month for each weekday and hour. Previous years were compared to the 2020 data to calculate the ratios. These ratios were then applied to scale the traffic emissions, applying the average reduction across the road transport sector. An average reduction was applied out of necessity, given that sufficient data to apply reductions in traffic by vehicle types and/or age was not available. Given that detailed data was not available, these ratios were assumed to be sufficiently representative for the change in road transport sector emissions and therefore applied to scale the traffic emissions in 2020. Furthermore, using hourly and day of week ratios ensured that, for example, Saturdays in March were reduced by the ratio characteristic for Saturday traffic count data in March from previous years relative to 2020 Saturdays in March, rather than a simple date comparison where the dates from previous years would not correspond to the same weekday in other years. This is relevant as patterns in traffic count data show substantial differences in weekdays in comparison to weekends.

2.2.2. Meteorological classification

A classification of synoptic meteorological patterns (SMP) was carried out for the region located between 40°W and 50°E and 20°N-80°N in the period January 2016–July 2020. To this end a non-hierarchical k-means cluster analysis method was applied for classifying sea level pressure (SLP) daily fields into similar groups, representing the main circulation types of air masses over central Europe. This is an iterative algorithm that partitions the data by comparing each object to each of the k cluster centers by a dissimilarity measurement. It is one of the statistical methods most widely used for classification of atmospheric circulation patterns (Huth et al., 2008 and references therein). Some recently published papers have demonstrated the robustness of the k-means cluster analysis method for characterizing atmospheric processes with high impact in air quality levels at a study area, such as long-range transport of African dust over regions of the western Mediterranean basin (Salvador et al., 2014), the transport and NO_2 background concentration over regions of the Iberian Peninsula (Valverde et al., 2015) or the development of high air pollution episodes and new particle formation processes in the Madrid metropolitan area (Salvador et al., 2021).

In fact Belis et al. (2019) recommended the use of classifications of atmospheric circulation patterns using SLP data fields, for discriminating periods under stagnant meteorological conditions, which usually lead to urban high-pollution episodes. In these cases high levels of NO_2 and of other air pollutants originated in local emission sources are frequently reached, giving rise even to exceedances of air quality guidelines. This is a highly relevant factor that should be taken into account in any study focused on urban air pollution like the present one.

First, SLP global fields at 12 UTC derived from the National Centre for Environmental Prediction/National Centre for Atmospheric Research (NCEP/NCAR) Reanalysis dataset (Kalnay et al., 1996) provided by NOAA/OAR/ESRL PSD, USA were obtained for all the days of the period of study. Data were distributed in each field in a 2.5° latitude x 2.5° longitude global grid. Those data contained in the region located between 40°W and 50°E and 20°N-80°N were downloaded, resulting in 925 SLP grid points for each daily field.

Then, the k-means cluster analysis was carried out. This method comprises 4 stages (Belis et al., 2019):

Stage 1: an initial partitioning of the SLP fields is defined: k daily fields representing different representative synoptic meteorological situations in the study area are selected as initial seeds or cluster centers. In this study the 8 synoptic meteorological scenarios obtained from a cluster analysis of back-trajectories performed in sites of central Europe by Salvador et al. (2010) were used as initial cluster centers. They represented the main atmospheric circulation patterns that occur over central Europe and showed a marked seasonal pattern, with fast westerly and northerly Atlantic flows developing during winter and weak circulation flows in summer. Spring and fall were characterised by advection of moderate flows from northeastern and eastern Europe.

Stage 2: calculate the change in the clustering criterion that result from changes in membership and reassign SLP fields. Hence, the Euclidean distance from each field j to each cluster-center k is calculated for every grid-point value of their 861 SLP observations and summed. Finally, the SLP field is assigned to the cluster with the smallest total distance from its cluster center.

Stage 3: recalculate the cluster centers after all the SLP fields have been examined and assigned. The cluster centers are recalculated as the arithmetic mean of all members of any cluster.

Stage 4: repeat the steps 2 and 3 iteratively until no SLP field changes its cluster assignment.

A script in FORTRAN was created to implement the non-hierarchical k-means cluster analysis, once it was performed, composite synoptic

maps were thus obtained by averaging all the SLP fields allocated in each group, grid-point by grid-point.

2.2.3. Air quality

Air pollutant observations were retrieved from all 16 monitoring stations that comprise the Berlin air quality monitoring network (Berlin Luftgüte Messnetz, BLUME) for the period 2016 through mid-2020. The data retrieved were hourly data for NO_2, O_3, and PM10. All measurements meet the criteria and guidelines set by the European Air Quality Directive (EC, 2015) and undergo quality checks before being officially reported and made public. Data coverage was greater than 90 % for all time periods included.

An initial analysis of air pollutant concentrations was carried out by monitoring site type (traffic, urban background, and city periphery). This analysis used the concentrations as given and did not account for meteorological influence, simply comparing median values and the differences in median values during the core lockdown period.

Subsequently, the median concentrations for each SMP during the lockdown period were calculated for 2020 and 2016–2019. Based on these SMP classified concentrations, ratios in the median NO_2 concentrations, as well as weighted mean and weighted standard deviations of the median NO_2 concentrations were calculated for the lockdown period in 2020 and 2016–2019. The weighting reflected the relative occurrence of the different SMP. Finally, when calculating the difference between the weighted averages to assess the change between 2020 and 2016–2019, the standard deviation was propagated as error. If the error overlapped with zero the differences were considered to be insignificant. Statistical significance between concentrations in 2020 and 2016–2019 were tested with the Wilcoxon-Mann-Whitney *U* test and the Kolmogorov-Smirnov test (results in SI). Previously stated data coverage conditions were met, with the exception of MC 174 (Frankfurter Allee) for which only 55 % of data were available for SMP 8 in 2020. This data was retained in the analysis, as it did not influence the overall outcome.

2.3. Modelling

The WRF-Chem model version 3.9.1 (Fast et al., 2006; Grell et al., 2005) was used to simulate the concentrations of trace gases and aerosols. For this purpose, we have set up two nested domains, using a 15 km grid spacing for a coarser domain that covers Europe, and 3 km grid spacing for an inner domain centred over Berlin. Previous work by Kuik et al. (2016) has shown that resolutions finer than a 3 km grid spacing over Berlin did not produce any significantly better model performance for simulation of the urban background concentrations of NO_x and O_3. Veratti et al. (2020) also showed that a grid having a spatial resolution of 3 km over Modena (Italy) is better suited to reproduce the observed NO_x concentration than a grid having 1 km resolution. The vertical coordinates use 35-sigma stretched levels, with a ~30 m above surface and 12 levels located within 3 km of the ground. The main physical and chemical model options selected for this study are listed in Table 2.

Table 2
Main physical and chemical options applied in the simulations.

Process/Variable	Option in WRF-Chem	Reference
Microphysics	Morrison double-moment scheme	Morrison et al. (2009)
Cumulus parameterization	Kain-Fritsch	Kain (2004)
Longwave radiation	Rapid Radiation Transfer Model	Mlawer et al. (1997)
Shortwave radiation	Dudhia scheme	Dudhia (1989)
Boundary layer parameterization	YSU scheme	Hong et al. (2006)
Surface layer scheme	Monin-Obukhov	Jimenez et al. (2012)
Gas-phase chemistry mechanism	MOZART	Pfister et al. (2011)
Aerosol module	GOCART	Chin et al. (2002)

Initial and boundary conditions for the meteorological parameters are taken from the ECMWF reanalysis. Biogenic trace gas emissions are calculated online using the MEGAN model (Guenther et al., 2006). Anthropogenic emissions of CO, NOx, SO_2, NMVOCs, PM10, PM2.5, and NH_3 are obtained from the 2015 CAMS regional emissions (CAMS-REG_v2.2.1) with spatial resolution of 6 km × 6 km,[3] the National emissions for Germany (UBA-GRETA) for 2015 at 1 km × 1 km horizontal resolution[4] and the highly resolved city of Berlin emissions for 2015 provided by the Berlin Senate. The lockdown emissions were calculated using a set of emission reduction factors for Europe computed at BSC (Guevara et al., 2020) that varies per day, country and sector. In addition, for the urban area of Berlin, we used hourly emission reduction factors for the traffic sector based on traffic counts, as described in section 2.b.i. The NOx emissions used in the model scenarios are shown in Fig. 1.

Previous work using the WRF-Chem model for Berlin has shown consistent underestimation of the observed concentrations of NOx (Kuik et al., 2018), and has linked this to a potential underestimation of NOx emissions from road transport. An underestimation of traffic NOx emissions in the inventories commonly used as input for modelling studies over Europe has also been identified in several other studies (e.g., Karl et al., 2017; Lee et al., 2015; Oikonomakis et al., 2018). In the present study, we use the unprecedented reduction in NOx emissions from the road transport sector during the COVID-19 lockdown as an additional test of the ability of the model to simulate the change in the ozone production regime associated with the emission reduction. A comparison of modelled and observed NO_2 and O_3 concentrations with the observations is shown in Figure S6.

3. Results

Given that almost all exceedances of NO_2 limit values occur at traffic air quality monitoring locations, and we are using the COVID-19 context to explore the potential of changes in traffic to influence air quality in the city, the focus in the analysis will be on these sites, within the broader context of changes across the city overall using the urban background stations. Furthermore, while we will briefly address changes in PM10 and O_3, as other studies have shown, and we also find, the largest changes are generally observed for NO_2 (e.g., Briz-Redón et al., 2021; Menut et al., 2020).

3.1. Traffic count data

Here we outline the results from the traffic count data from four traffic counting and air quality monitoring sites. The change in traffic counts at these stations is shown in Table 3. As demonstrated by this data, there was a substantial decrease in passenger car traffic and a somewhat lesser decrease in truck traffic. Overall, total traffic counts are dominated by passenger car counts. Trucks represent only 3 to 10 % of the total counts at any of the sites. The reductions in passenger car traffic ranged from 31 to 44 %, while truck traffic decreases ranged from 7 to 38 % during the core lockdown period in 2020 relative to the same period in 2016–2019. Overall, the total vehicle count across all four sites during the core lockdown period was 36 % lower in 2020 compared to the previous four-year average. In addition, reductions in vehicle counts were 10 to 16 % greater on weekends than during weekdays. This reflects the greater restrictions with respect to the travel freedom of individuals. We assume that any changes in traffic counts related to weather are negligible.

[3] https://eccad3.sedoo.fr/.
[4] https://www.umweltbundesamt.de/deutschland-karten-zu-luftschadstoff-daten#undefined.

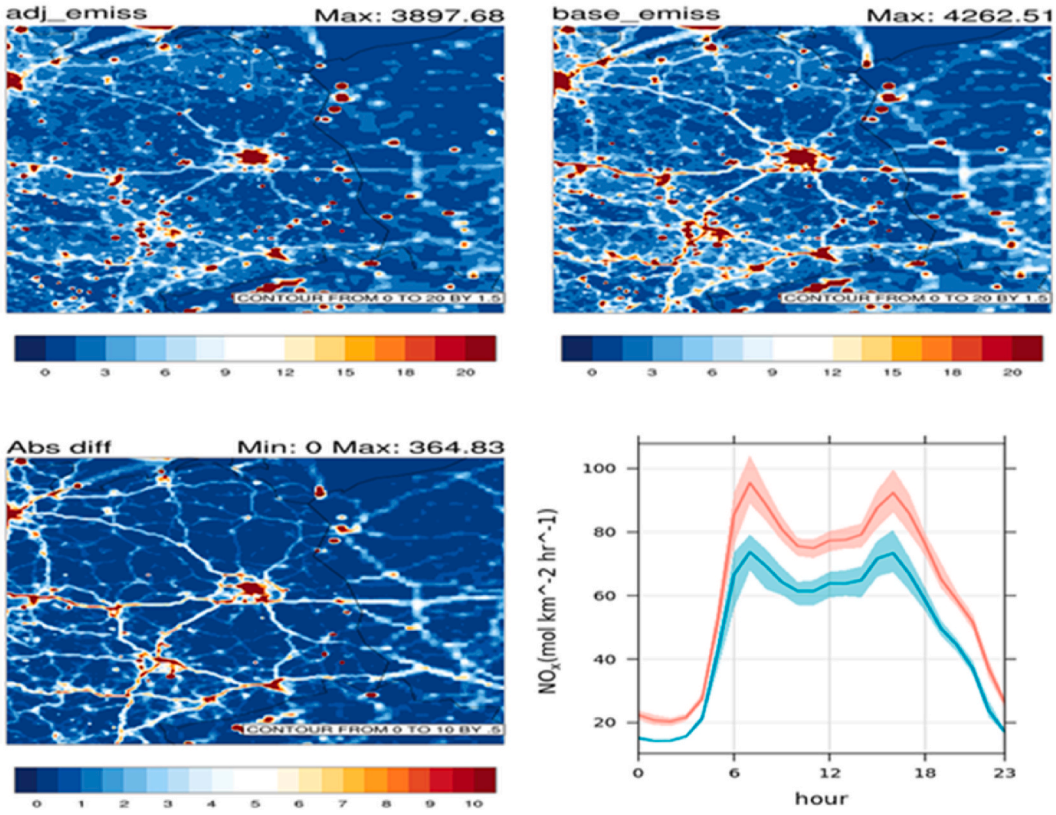

Fig. 1. Total NOx emissions (mol km^{-2} hr^{-1}) used in the model from all source sectors for the base run (top right), the 'lockdown' run (top left), and the difference (bottom left) in the emissions, as well as the diurnal cycle (bottom right) for the base run (red) and lockdown run (blue). (For interpretation of the references to colour in this figure legend, the reader is referred to the Web version of this article.)

Table 3
Changes (%) in traffic counts during the full lockdown period at four traffic count stations in Berlin. 2020 changes are calculated compared to 2016–2019 averages. Upper and lower bounds based on 95 % confidence intervals.

Station	Passenger Cars		Trucks		Total	
	Weekday	Weekend	Weekday	Weekend	Weekday	Weekend
Schildhornstrasse	41 (38; 44)	52 (49; 54)	23 (16; 30)	23 (11; 32)	40 (37; 42)	50 (47; 53)
Mariendorfter Damm	31 (28; 34)	46 (44; 49)	6 (-3; 13)	11 (-2; 21)	30 (27; 32)	45 (42; 47)
Frankfurter Allee	33 (31; 36)	49 (46; 52)	33 (25; 40)	49 (32; 59)	33 (31; 36)	49 (46; 52)
Karl-Marx-Strasse[a]	27 (22; 31)	43 (39; 46)	19 (4; 29)	36 (19; 47)	26 (21; 30)	42 (38; 46)
Average	33 (30; 36)	47 (44; 50)	20 (11; 28)	29 (15; 40)	32 (29; 35)	47 (43; 49)

[a] The changes for Karl-Marx-Strasse are calculated compared to 2019 values only owing to construction that changed the pattern of the street and reduced traffic in 2019 relative to 2016–2018.

3.2. Meteorological classification

Eight SMP were obtained, which represent the average situation at 12 UTC during any day of each cluster. They are shown in Fig. 2. In addition, the main features of each SMP are summarized in Table 4. Their main features and prevailing seasonal development resemble very well with those determined in the study of Salvador et al. (2010). For more information on the meteorological classification and the impact of the different SMP on the mean levels of air pollutants in Berlin see Section S2 in the supplemental information. These results strongly suggest that the SMP were correctly identified. Namely, the highest levels of primary anthropogenic air pollutants, NO, CO and NO_2 were registered during days under meteorological situations characterized by the presence of high-pressure systems in winter and autumn (SMP-2 and SMP-3). Otherwise, the highest daily mean levels of O_3 were obtained during those SMP that were more frequently produced in the spring and summer periods and had associated the lowest levels of NOx (SMP-4, SMP-5 and SMP-7).

The fraction of days during the core lockdown period that corresponded to the different SMP is also shown in Table 4. Comparing 2016–2019 with 2020, we see some similarities in that the overall SMPs 1 through 4 are less prevalent, and that SMPs 5 through 8 are more prevalent during both time periods. For both, SMP 8 is the most common with 33 % and 39 % of days for 2016–2019 and 2020, and occurrence of SMP 6 is similar, with 14 % and 12 %, respectively. For SMP 5 we see a greater prevalence in 2020, accounting for 24 % of days (10 % in 2016–2019) and a greater prevalence for SMP 7 during the 2016–2019 period with 31 % of days (10 % in 2020).

3.3. Air quality (without consideration of meteorology)

The median air pollutant concentrations and the simple difference in medians by site type are summarized in Table 5 and S1 respectively. It is worth noting that generally, for all site types, the concentrations in 2019 are substantially lower (higher) than the previous years for NO_2 (O_3). Despite gradual changes in air pollution concentrations over the years,

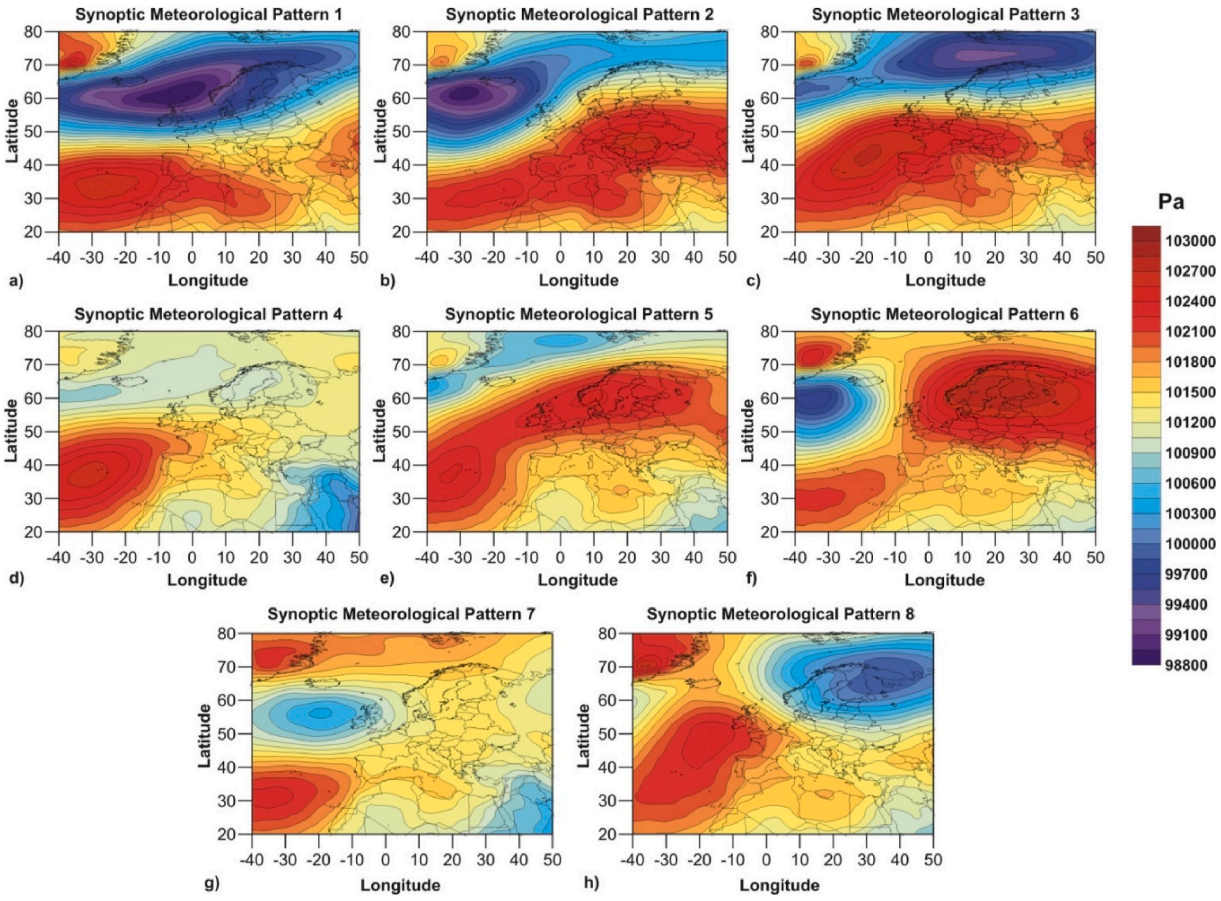

Fig. 2. Synoptic meteorological patterns (SMP) resulting from the circulation classification procedure applied to sea level pressure fields at 12 UTC for the period Jan 2016–Jul 2020.

Table 4
Meteorological classifications.

SMP	Main features	Seasonal development	Fraction of days between 24 March and 21 April 2016-19 and 2020	
1	Strong baric gradient across western, central and northern Europe. Fast W flows.	Winter	0.01	0
2	High pressures in central Europe. Slow SE-SW flows.	Winter/Autumn	0.03	0.04
3	High pressures in western Europe extended across France and Germany. Slow NW flows.	Winter/Autumn	0.03	0.08
4	Weak baric gradient over central and eastern Europe. Slow W flows.	Summer	0.05	0.03
5	High pressures in northern Europe. Moderate N-NE flows	Spring/Autumn	0.10	0.24
6	High pressures in northern Europe extended towards the E. Moderate E flows.	Autumn/Spring	0.14	0.12
7	Weak baric gradient over central and eastern Europe. Moderate S flows at the 850 mb level.	Spring/Summer	0.31	0.10
8	Strong baric gradient across N Europe. Fast NW-N flows.	Spring/Autumn	0.33	0.39

Table 5
Median air pollutant concentrations over the 22 March – 21 April time period by year.

	2016	2017	2018	2019	2016–2019 avg	2020
Traffic NO_2 (n = 5)	49.4	44.2	43.0	30.2	41.6	22.0
Traffic NO_2 (n = 4)[a]	49.5	45.5	42.0	30.0	41.8	23.5
Urban Background NO_2	23.7	21.2	21.0	16.0	20.4	11.6
City Periphery NO_2	10.2	9.0	10.1	8.6	9.2	6.2
Traffic PM10	22.8	23.6	31.3	25.6	25.6	20.8
Urban Background PM10	18.0	18.0	24.2	21.3	20.7	16.7
City Periphery PM10	14.7	14.7	21.0	19.0	17.3	15.7
Traffic O_3	–	–	–	63.0	63.0	69.0
Urban Background O_3	51.5	56.5	58.5	67.0	58.5	72.5
City Periphery O_3	58.5	65.1	63.0	70.2	64.6	74.6

[a] Limited to the four traffic air quality monitoring stations where traffic counts were also measured.

which can be linked to the implementation of emission reduction policies, the difference in 2019 relative to previous years is a larger change, which also demonstrates the influence of meteorology in determining pollutant concentrations (in addition to the influence of ongoing policy measure developments). More specifically, in 2019, a disproportionately large amount of 'clean' air masses originated from the north were observed during winter and spring (more days under SMP 7, and to a certain extent under SMP 1 and SMP 6), which was not typical of any of the other years. This difference in meteorological conditions over Europe in 2019 has also been noted by other studies (Barré et al., 2020). This is carried through and is also visible in the simple differences in medians (Table S1), where the reductions (increases) in NO_2 (O_3) that are observed are much smaller for 2019–2020 in comparison to earlier

years. Furthermore, the PM10 concentrations in 2018 are also higher than in the other years. Considering 2016–2019 as the baseline for comparison rather than individual years, at the four air quality traffic stations that also have count data, a reduction in the median concentration of 18 μg m^{-3} is observed for NO_2. However, while there is a general consistency in concentrations across years, some of the larger differences indicate the necessity of accounting for the influence of meteorology. Through subsetting into similar SMP we assume that the NO_2 stability dependence on solar radiation is accounted for.

3.4. Air quality observations (accounting for meteorological influence)

3.4.1. Nitrogen dioxide

The comparison of air pollutant concentrations at traffic sites in Berlin, grouped by the SMP, is shown in Fig. 3 (weekdays) and Fig. 4 (weekend days). Across all synoptic conditions, with the exception of weekend values at the Frankfurter Allee station for SMP6, Figs. 3 and 4 show reductions in NO_2 in 2020 relative to the same time period for the previous years. Comparing the median ratios of NO_2 concentrations in 2020 relative to the previous years by SMP, we see that the range of ratios for the four traffic sites is 0.10 to 0.92 on weekdays and 0.25 to 1.1 on weekends (Table S2). For interpreting the ratios, the closer to 1 the more similar 2020 values were to the previous four years. The differences in median concentrations for the 2020 lockdown period to the previous years have quite a large range, showing reductions from 3 to 55 μg m^{-3} for weekdays and -2 to 28 μg m^{-3} for weekends across the four traffic sites. (Negative values in this case represent an increase relative to previous years.) As a weighted average, with weighting corresponding to prevalence of the SMP, the difference between 2020 during the lockdown period and the previous four years during the same period ranged from 15 to 22 μg m^{-3} on weekdays and 9.0 to 17 μg m^{-3} on weekends (see Table 6). Overall, the average 33 % (47 %) reduction in passenger car traffic and 20 % (29 %) reduction in truck traffic, lead to 39 % (42 %) reductions in SMP-weighted NO_2 concentrations during weekdays (weekends).

The changes in the observational data from the five urban background monitoring stations are shown in Table 7. These reflect the SMP-weighted changes in NO_2 concentrations. The observed reductions ranged from 34 to 54 % on weekdays and 16 to 41 % on weekends.

3.4.2. Ozone

The SMP-weighted average of the median concentrations for ozone for the 2020 lockdown period compared to previous years is shown in Table 8. Only one traffic station had ozone data, and the change observed between both periods was not significant. Ozone showed an increase (20 % and 24 %) in concentrations in 2020 relative to the earlier years during weekdays at the two urban background monitoring stations where data was available. The weekend data showed no real change at the urban background stations, despite the observed decrease in NO_2 at urban background stations on weekends. The increase in O_3 (at least for weekdays) is likely a result of a reduction in the NO titration effect (that is, the consumption of O_3 that takes place in urban areas as a result of the titration reaction with the emitted NO to form NO_2 and O_2), where owing to the reductions in NOx emissions, an increase in O_3 results. This weekday weekend difference in O_3 could be owing to a number of factors. For one, the smaller NOx peak during the morning hours on the weekend may mean that ozone production is less inhibited than on weekdays and therefore allows greater ozone formation (Blanchard et al., 2008). For two, we do not have information on the changes in non-methane volatile organic compounds, that also play a crucial role in ozone photochemistry and could be affecting this difference. However, local photochemistry at this time of year would likely be somewhat more limited, indicating that a combination of changes in the regional background and local titration are more plausible explanations. Finally, Guevara et al. (2020) found that in Paris and Berlin, non-traffic sources contributed ca. 23 % to total NO_2 reductions; these non-traffic sources with substantial contributions to total emissions included power generation, and to a lesser extent industry and other stationary combustion. There were lesser reductions in these sectors with different weekday-weekend patterns that could also affect the subsequent difference in O_3 concentrations.

3.4.3. Particulate matter

At the four traffic and three urban background monitoring stations where PM10 data was available, a reduction in concentrations was observed in 2020 relative to the earlier years (Tables S3 and S4).

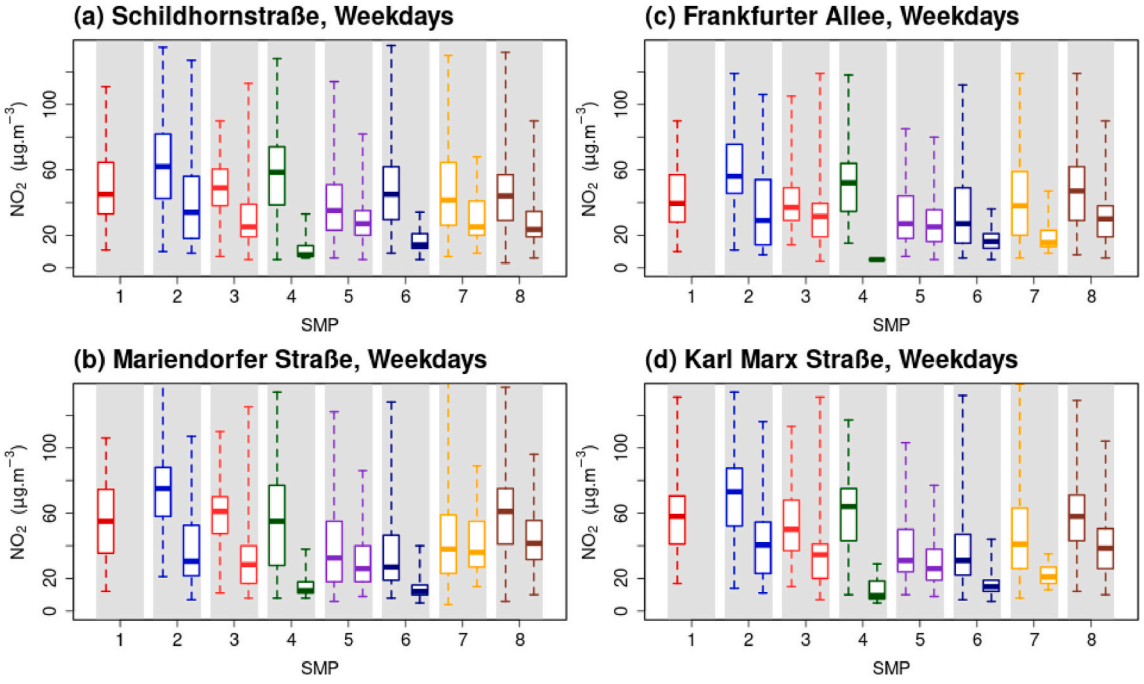

Fig. 3. Observed NO_2 weekday concentrations from 22 March – 21 April in 2016–2019 (left box & whisker within gray bar) and 2020 (right box & whisker within the same gray bar) classified by SMP for the four air quality monitoring stations corresponding to the traffic count stations.

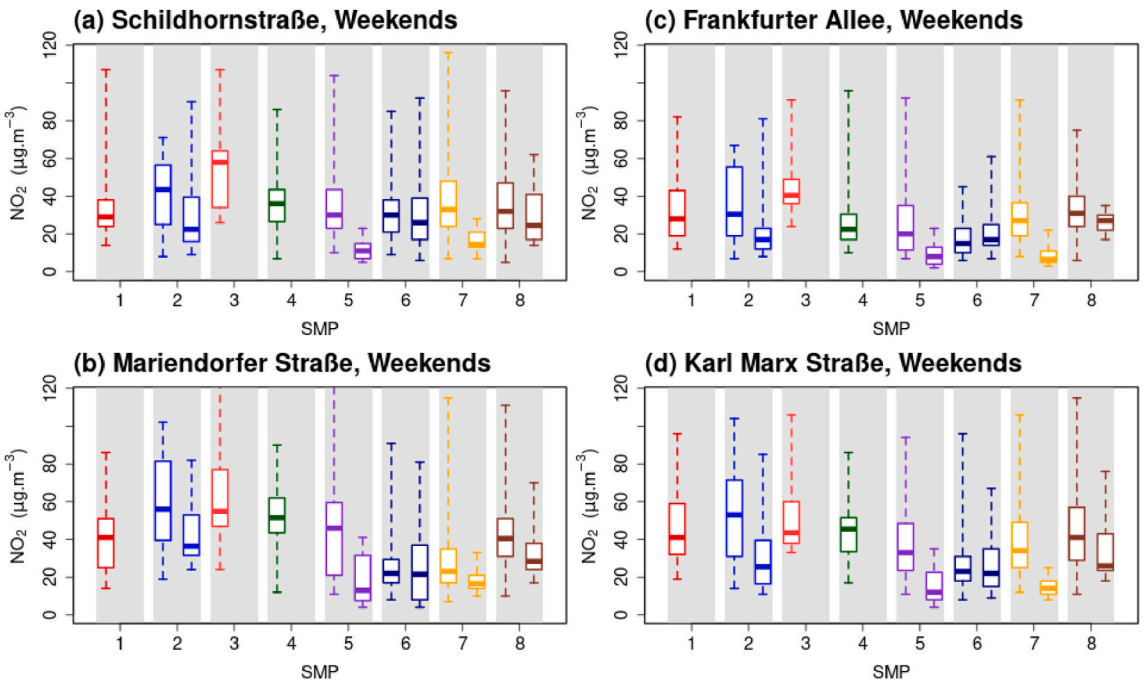

Fig. 4. Observed NO_2 weekend concentrations from 22 March – 21 April in 2016–2019 (left box & whisker within gray bar) and 2020 (right box & whisker within same gray bar) classified by SMP for the four air quality monitoring stations corresponding to the traffic count stations.

Table 6
Weighted mean and weighted standard deviation of the **median NO_2** concentrations (µg m^{-3}) during the 2020 lockdown period (22 March – 21 April) compared to 2016–2019 averages, as well as difference (2016–2019 minus 2020), for the four air quality stations corresponding to the **traffic** count locations across all SMP. Weighting is based on the prevalence of the different SMP. Stdev was propagated as error. Percent change shown as a reduction in 2020 relative to earlier years; not shown if error overlaps with zero. Negative difference and % change values indicate an increase.

Station	Weekdays				Weekends			
	2016–2019	2020	Diff.	% Change	2016–2019	2020	Diff.	% Change
Schildhorn-strasse	44 ± 5.4	23 ± 5.0	22 ± 7.4	49	32 ± 5.5	18 ± 8.6	15 ± 10	45
Mariendorfter Damm	46 ± 14	32 ± 10	15 ± 17	–	32 ± 11	20 ± 9.8	12 ± 15	–
Frankfurter Allee	40 ± 8.5	24 ± 7.0	16 ± 11	32	25 ± 6.9	16 ± 10	9.0 ± 12	–
Karl-Marx-Strasse	47 ± 12	29 ± 9.3	18 ± 15	37	35 ± 7.5	18 ± 8.7	17 ± 11	48

Table 7
Weighted mean and weighted standard deviation of the **median NO_2 concentrations** (µg m^{-3}) during the 2020 lockdown period (22 March – 21 April) compared to 2016–2019 averages, as well as difference (2016–2019 minus 2020), for the five **urban background** (ub) and three **rural** (r) air quality stations across all SMP. Weighting is based on the prevalence of the different SMP. Stdev was propagated as error. Percent change shown as a reduction in 2020 relative to earlier years; not shown if error overlaps with zero. Negative difference and % change values indicate an increase.

Station	Weekdays				Weekends			
	2016–2019	2020	Diff.	% Change	2016–2019	2020	Diff.	% Change
Wedding (ub)	24 ± 5.2	16 ± 4.1	8.3 ± 6.6	34	19 ± 5.9	15 ± 8.0	4.2 ± 9.9	22
Schöneberg (ub)	20 ± 3.0	13 ± 3.2	7.5 ± 4.4	37	18 ± 3.5	12 ± 5.6	5.4 ± 6.6	30
Neukölln (ub)	21 ± 3.2	12 ± 3.1	8.8 ± 4.4	42	16 ± 3.0	14 ± 8.0	2.6 ± 8.5	16
Mitte (ub)	22 ± 4.9	9.9 ± 2.4	12 ± 5.4	54	17 ± 4.5	10 ± 5.7	6.9 ± 7.2	41
Karlshorst (ub)	16 ± 3.5	10 ± 2.8	6.4 ± 4.4	39	12 ± 2.9	10 ± 5.7	1.9 ± 6.4	16
Hasenholz (r)	8.2 ± 1.3	6.6 ± 2.0	1.6 ± 2.3	–	7.4 ± 1.3	5.4 ± 1.5	2.0 ± 2.0	27
Lütte (r)	5.7 ± 0.74	4.1 ± 0.88	1.6 ± 1.2	28	5.0 ± 1.2	3.2 ± 1.1	1.8 ± 1.7	36
Neuglobsow (r)	2.6 ± 0.72	2.0 ± 0.28	0.59 ± 0.77	–	2.8 ± 0.55	2.0 ± 0.0	0.79 ± 0.55	28

However, the differences are not significant in that the standard deviation propagated as error indicates an overlap with zero.

3.5. Model results and comparison with observations

The WRF-Chem modelled NO_2 concentrations for the lockdown period are shown in Figure S1. The model generally underestimates the observed NO_2, while the morning peaks are underestimated, and the evening peaks are sometimes missed. The overall underestimation by WRF-Chem of NO_2 in Berlin has been noted in previous work (Kuik et al., 2018). Consistent with the modelled results for NO_2, the model somewhat overestimates ozone relative to the observations at the urban background sites, although the diurnal cycle is captured well (Figure S2). The over- or underestimates, however, will be consistently carried through both scenarios and therefore should not have a large influence on the estimated change in concentrations. Evaluation of

Table 8
Weighted mean and weighted standard deviation of the **median O_3** concentrations (μg m^{-3}) during the 2020 lockdown period (22 March – 21 April) compared to 2016–2019 averages, as well as difference (2016–2019 minus 2020), for the **urban background** (ub) and **rural** (r) air quality stations across all SMP. Weighting is based on the prevalence of the different SMP. Stdev was propagated as error. Percent change shown as a reduction in 2020 relative to earlier years; not shown if error overlaps with zero. Negative difference and % change values indicate an increase.

Station	Weekdays				Weekends			
	2016–2019	2020	Diff.	% Change	2016–2019	2020	Diff.	% Change
Wedding (ub)	58 ± 7.8	72 ± 5.7	-14 ± 9.7	-24	64 ± 12	64 ± 23	0.69 ± 26	–
Neukölln (ub)	62 ± 5.7	74 ± 4.2	-12 ± 7.1	-20	64 ± 9.6	65 ± 23	-0.38 ± 25	–
Hasenholz (r)	65 ± 6.0	74 ± 6.7	-9.7 ± 9.0	-15	67 ± 5.2	79 ± 6.2	-12 ± 8.0	-17
Lütte (r)	64 ± 8.0	75 ± 5.1	-11 ± 9.5	-17	62 ± 11	76 ± 4.8	-14 ± 12	-23
Neuglobsow (r)	69 ± 8.8	79 ± 5.6	-9.7 ± 11	–	71 ± 11	76 ± 8.5	-5.0 ± 14	–

modelled concentrations against observations using statistical scores including mean bias (MB), normalized mean bias (NMB) and the correlation factor between simulated and measured values (R) is presented in the supplementary material (please see Section S3, including Table S7 and the subsequent discussion). In this work, we focus on comparison of the modelled changes in pollutant concentrations with the observed changes, rather than absolute concentrations.

The modelled changes in NO_2 concentrations, which represent changes in the urban background over the city (rather than at traffic sites), are summarized in Table 9 for the five urban background monitoring locations in Berlin and shown in Fig. 5. The model results show the change between a business-as-usual case and the 2020 lockdown case where emissions were scaled to reflect changes in traffic, and other sectors, resulting from the lockdown policies implemented. The changes in traffic for the urban area of Berlin were scaled based on observed changes in the traffic counts in the city (see methods section). While the model results showed percentage reductions in urban background median NO_2 concentrations consistent with the reduction in traffic counts, none were statistically significant due to the large model underestimation of the urban background NO_2 itself (Table 9). The difference in reductions modelled during the week and on weekends was minor.

When comparing the observations to the model results for NO_2, the observed changes generally show greater reductions during weekdays, and overall larger ranges than those in the model results. This is likely at least in part because reductions in traffic emissions for the model simulations were applied uniformly across the city.

In terms of the modelled change in ozone (Fig. 5), data were extracted for the two urban background monitoring sites where observational data is also available (Table 10). The model simulates a small (about 3 μg m^{-3}) decrease in ozone in the lockdown-adjusted 2020 simulation compared with the BAU simulation at urban background and nearby rural background stations. The modelled changes were not significant. There was no difference in the modelled reductions on weekdays versus weekends. These results contrast those from the observations (Table 8), where increases in O_3 were observed at the two urban background sites (20 and 24 %) on weekdays and no changes observed on the weekends. The lack of a strong increase in modelled ozone, as well as the lack of a weekday/weekend effect in either the change in simulated ozone or the absolute amount of simulated ozone is consistent with the model incorrectly simulating the ozone chemical regime. The model fails to simulate the NOx-saturated (ozone titrating) chemical regime which is indicated by the observations. The model failure to simulate NOx saturated conditions is consistent with the model underestimation of observed NO_2 (Figure S1 and previous work by Kuik et al., 2018) and the model overestimation of ozone (Figure S2). Kuik et al. (2018) showed that emissions of NOx from the road traffic sector in Berlin could be underestimated by up to a factor of 3.

The small decrease in modelled urban and rural background ozone under lockdown is consistent with the broader reduction in the simulated regional background ozone concentration (Fig. 5), which is itself consistent with the Europe-wide reduction in ozone precursor emissions (Guevara et al., 2020) as well as a general reduction in global hemispheric background ozone during the lockdown period (Steinbrecht et al., 2021). The reduction in rural background ozone near Berlin is not observed in the SMP-adjusted observations at rural background monitoring sites (Table 8).

4. Discussion

As highlighted by previous studies, ignoring the influence of meteorological factors when attributing air quality changes to COVID-19 policies (reductions in traffic) can substantially influence the estimated change (e.g. Barré et al., 2020; Petetin et al., 2020). For this reason, we focus only on the meteorologically adjusted observations and model results from our study and results from literature studies that similarly account for this in the context of the discussion.

An analysis of the emission changes in Europe owing to the COVID-19 lockdown measures showed that changes in urban NO_2 emissions were dominated by the changes in traffic. While changes in traffic still dominated for Berlin, Guevara et al. (2020) found that ca. 23 % of total NO_2 reductions observed in their analysis were from non-traffic sources (similarly so for Paris), which was a higher contribution from non-traffic sources than most other cities evaluated. The speed of reductions also varied, in that abrupt drops in NO_2 concentration were observed in

Table 9
Median and standard deviation of the **modelled NO_2 concentrations** (μg m^{-3}) during the 2020 lockdown period (22 March – 21 April), for a business as usual (BAU) case and 2020, reflecting the changes in emissions owing to lockdown policies, for the five **urban background** (ub) air quality stations in Berlin and three **rural** (r) air quality stations outside the city. Negative difference and % change values indicate an increase.

Station	Weekdays				Weekends			
	BAU	2020	Diff.	Percent change	BAU	2020	Diff.	Percent Change
Wedding (ub)	6.3 ± 4.6	3.9 ± 3.4	2.4 ± 5.7	–	5.2 ± 4.4	3.2 ± 3.2	1.9 ± 5.4	–
Schöneberg (ub)	8.3 ± 4.9	5.8 ± 3.5	2.5 ± 6.0	–	6.6 ± 4.7	4.1 ± 3.4	2.5 ± 5.8	–
Neukölln (ub)	7.0 ± 5.4	5.1 ± 3.9	2.0 ± 6.7	–	4.4 ± 4.8	3.0 ± 3.6	1.4 ± 6.0	–
Mitte (ub)	5.8 ± 4.7	4.3 ± 3.4	1.5 ± 5.8	–	3.5 ± 4.6	2.5 ± 3.6	1.1 ± 5.8	–
Karlshorst (ub)	6.2 ± 5.3	4.6 ± 4.2	1.5 ± 6.7	–	3.9 ± 4.2	2.7 ± 3.1	1.2 ± 5.2	–
Hasenholz (r)	3.1 ± 4.2	1.9 ± 2.4	1.2 ± 4.8	–	2.0 ± 2.6	1.9 ± 2.2	0.10 ± 3.4	–
Lütte (r)	3.4 ± 3.2	2.0 ± 1.9	1.4 ± 3.7	–	2.7 ± 3.0	1.6 ± 1.8	1.1 ± 3.5	–
Neuglobsow (r)	2.6 ± 2.4	1.5 ± 1.7	1.2 ± 3.0	–	1.6 ± 3.3	1.0 ± 1.4	0.61 ± 3.6	–

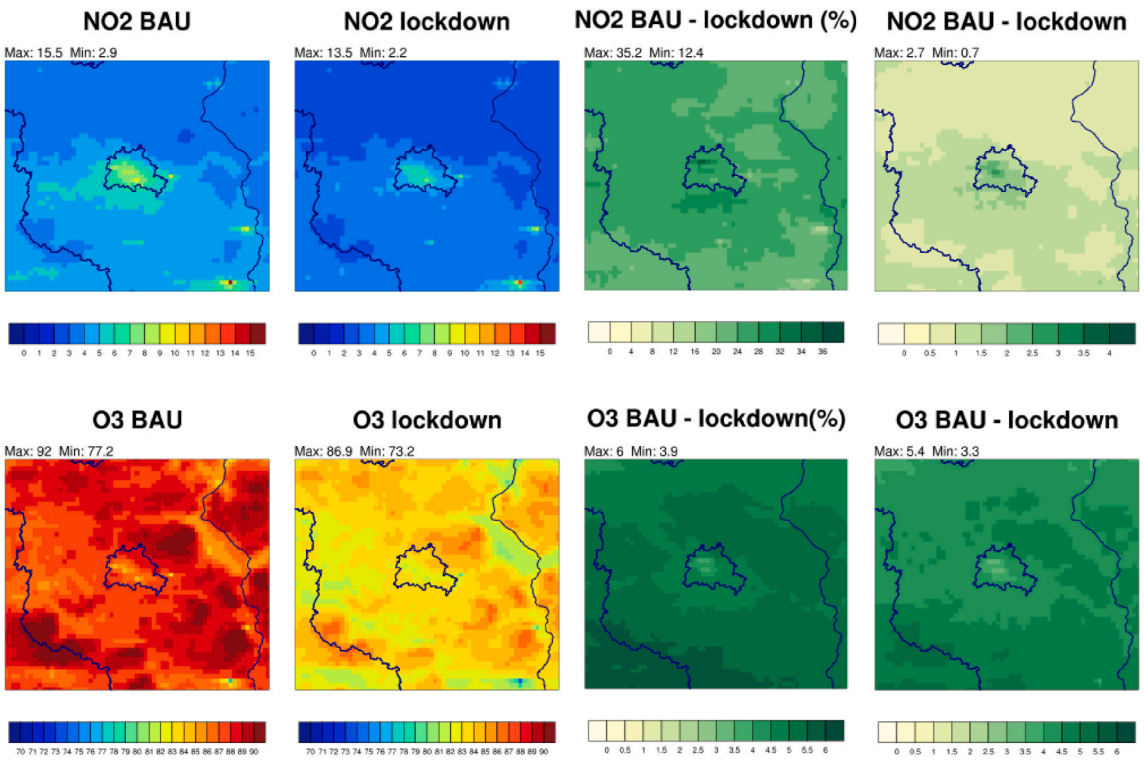

Fig. 5. Modelled concentrations of NO2 (top row) and O3 (bottom row), including (from left to right) the business-as-usual scenario, the lockdown scenario, the difference in concentration as a percent, and the difference in concentration as an absolute value.

Table 10
Median and standard deviation of the **modelled O_3 concentrations** (μg m^{-3}) during the 2020 lockdown period (22 March – 21 April), for a business as usual (BAU) case and 2020, reflecting the changes in emissions owing to lockdown policies, for the two **urban background** (ub) air quality stations in Berlin and three **rural** (r) air quality stations outside the city. Negative % change values indicate an increase.

Station	Weekdays				Weekends			
	BAU	2020	Diff.	% Change	BAU	2020	Diff.	% Change
Wedding (ub)	92 ± 15	89 ± 13	3.0 ± 20	–	95 ± 19	92 ± 18	3.7 ± 26	–
Neukölln (ub)	92 ± 15	88 ± 13	3.7 ± 20	–	96 ± 20	92 ± 18	3.6 ± 27	–
Hasenholz (r)	94 ± 16	91 ± 14	2.8 ± 21	–	98 ± 18	95 ± 20	3.0 ± 27	–
Lütte (r)	95 ± 15	94 ± 14	1.2 ± 21	–	98 ± 19	99 ± 19	-1.2 ± 27	–
Neuglobsow (r)	94 ± 13	93 ± 15	1.0 ± 20	–	97 ± 16	100 ± 19	-3.0 ± 24	–

Madrid and Paris, whereas the decreases were somewhat more gradual in Milan, Berlin, and London (Guevara et al., 2020).

Generally, the largest reductions were observed in urban areas across Europe. Briz-Redón et al. (2021) estimated reductions in NO_2 levels of ca. 20 μg m^{-3} or more across 10 cities in Spain during their major lockdown period. Petetin et al. (2020) also evaluated changes in NO_2 at ca. 50 urban background and traffic monitoring sites across Spain using a machine learning model and attributed a ca. 50 % reduction to the lockdown measures on average; for Madrid the reductions were -39 % (-14 μg m^{-3}) at urban background locations and -59 % (-20 μg m^{-3}) at traffic locations, similar to results of Briz-Redón et al. (2021). Barré et al. (2020) estimated median reductions in NO_2 levels between ca. 20 and 40 % depending on the methodology used, including satellite total column estimates, modelled estimates, and machine learning estimates based on both observational and satellite data, during the core lockdown period. Grange et al. (2020) used machine learning to compare a counterfactual, business-as-usual air quality time series to changes during the 2020 lockdown during maximum restrictions on mobility across 102 urban areas in 34 countries in Europe. They found that NO_2 decreased on average 34 % (-11 μg m^{-3}) at traffic and 32 % (-7 μg m^{-3}) at urban background locations. Furthermore, their estimates for NO_2 reductions for urban areas across Germany were -29.3 % (10.5 μg m^{-3}) at traffic sites and -21.6 % (-4.9 μg m^{-3}) at urban background sites. Menut et al. (2020) conducted a model analysis using WRF-CHIMERE to compare March 2020 with and without lockdown measures, finding slightly lesser reductions in NO_2 in Germany and the Netherlands (-15 to -30 %), relative to the other European countries evaluated (-35 to -45 %). Finally, Ordóñez et al. (2020) used a generalized additive model to evaluate changes in observed daily maximum NO_2 concentrations over Europe and found reductions that ranged from 5 to 55 % for the vast majority of the sites, attributing the changes to reductions in emissions. For those studies that looked at multiple countries in Europe, somewhat smaller reductions were fairly consistently observed for Germany relative to some of the other countries, such as Italy or Spain (Grange et al., 2020; Guevara et al., 2020; Menut et al., 2020; Ordóñez et al., 2020). The reductions observed for NO_2 in this study are generally in line with those observed in the literature.

Some of the studies also evaluated changes in ozone and/or PM. For PM, similarly to the changes estimated here, some reductions were observed but these were generally much smaller in magnitude than for NO_2 and in many cases not significant, likely owing to a much greater diversity of sources, apart from road traffic (Briz-Redón et al., 2021;

Menut et al., 2020). Menut et al. (2020) observed substantial increases in ozone in urban areas (-2.7 % to 17.6 %) and slight reductions in rural areas (-2.45 % to 6.60 %) across Europe (reported as national averages); 4.5 % and 0.73 % increases for urban and rural areas of Germany. The reductions of ozone in rural areas are consistent with a general reduction in background ozone during spring of 2020 (Steinbrecht et al., 2021). Springtime ozone in Europe is strongly linked with long-range transport of hemispheric background ozone (Butler et al., 2020; Jonson et al., 2018). Grange et al. (2020) observed increases in ozone of 30 % (12 μg m^{-3}) at traffic sites and 21 % (9 μg m^{-3}) at urban background sites across Europe. For Germany, they estimated an increase in O_3 of 37.3 % (15.1 μg m^{-3}) at traffic sites and 16.6 % (8.8 μg m^{-3}) at urban background sites, which is somewhat higher than the estimates of Menut et al. (2020) but likely explained by methodological differences in the focus areas (specific monitoring sites versus urban vs rural classification of modelled grid cells). Finally, Ordóñez et al. (2020) found that O_3 decreased over the Iberian Peninsula but increased elsewhere in Europe, with 10–22 % increases in O_3 at urban background stations in North-western and Central Europe. In this study we estimated increases in weekday O_3 at urban background sites in Berlin of ca. 22 % and no change on weekends; the modelled results showed no significant changes at urban background locations, consistent with the large model underestimation of urban background NO_x also noted in earlier work (Kuik et al., 2018). The other studies did not evaluate changes in observed concentrations for weekdays versus weekends. In the urban areas, the ozone increases are largely attributed to a decrease in the NO titration effect owing to the reductions in NOx emissions from traffic (Grange et al., 2020; Ordóñez et al., 2020; Sicard et al., 2020b). Grange et al. (2020) also investigated the overall change in Ox concentrations (NO_2 + O_3), finding that Ox concentrations remained constant. This indicates that the reductions in NO_2 were balanced out by increases in O_3, which has substantial policy implications, which led them to the conclusion that in order to not replace one air quality issue with another, if NOx reductions are to be continued, parallel reductions in NMVOCs will need to be carried out to avoid substantial increases in ozone, which are also associated with adverse health effects. Ordóñez et al. (2020) also point out that reduced aerosol loadings during the lockdowns could have led to O_3 enhancements thru increased photolysis rates and/or diminished uptake of HO_2 radicals that remove NO from the atmosphere. Other research has also found that higher ozone concentrations in cities during the weekend could be attributed to higher solar radiation favoring ozone formation in the context of lower aerosol loadings (Sicard et al., 2020a). In the analysis by Ordóñez et al. (2020) they found that meteorological conditions played a substantial role in explaining a large proportion of the observed changes in ozone; hypothesizing as well that changes in O_3 patterns could be analogue to evaluating pollution control policies under climate change scenarios.

5. Conclusions

Here we analysed observational traffic count and air quality monitoring data, accounting for meteorological conditions, and applied the WRF-Chem model with higher resolution over Berlin to evaluate changes in NO_2, O_3, and PM as a result of lockdown policies associated with the COVID-19 pandemic during the initial lockdown period in Spring of 2020. In Berlin, Germany, traffic counts decreased by 32 % and 47 % on average for weekdays and weekends, respectively, during the core lockdown period from 22 March – 21 April in 2020 relative to 2016–2019. Corresponding reductions in median observed NO_2 concentrations of averaged 40 % (42 %) at traffic stations and 41 % (25 %) at urban background stations for weekdays (weekends), while modelled reductions in median NO_2 concentrations were not significant at urban background stations. This change in the observed data is in line with previously published studies. For ozone, an increase of ca. 22 % in the measured urban background was found for weekdays, while no significant change was observed for weekends. The model results showed no significant change for weekdays or weekends. The discrepancy between modelled and measured ozone concentration, and the lack of a simulated weekday/weekend effect is consistent with the model failing to simulate a NOx-saturated chemical regime for ozone production. This is itself consistent with previous work suggesting that NOx emissions from traffic could be significantly underestimated in Berlin and other European cities. The difficulty of models in simulating urban background NO_x concentrations and the associated ozone chemical regime should be addressed in future work in order for models to be used as more effective tools for assessing future reductions in urban NO_x emissions.

These results indicate the potential for improvements in air quality due to policies for reducing traffic, along with the scale of reductions that would be needed to result in meaningful changes in air quality if a transition to sustainable mobility is to be seriously considered. They also confirm once more the highly relevant role of traffic for air quality in urban areas. What these results also highlight is the complexity of atmospheric chemistry and the potential danger of making progress on one air quality issue – i.e., NO_2 – and subsequently replacing it with a different air quality issue – i.e., O_3. To avoid this, reductions in NMVOCs will be needed in parallel (Grange et al., 2020), although this may not be adequate in some regions and seasons, due to the increasing importance of regional background ozone for the exposure of urban populations, especially in the springtime. The lack of measurements focused on NMVOCs (and therefore also the lack of analysis in the literature that considers this in this context) highlights a substantial gap in observations. Future analysis should, to the extent possible, aim to address this. Furthermore, additional measurement of NMVOCs should be considered and implemented where possible, given the complexity of the relationship and need for understanding a wide range of aspects of these related pollutants. Finally, these results also demonstrate that a reduction in traffic will not sufficiently address the issue of particulate matter, for which a greater diversity of sources will have to be considered.

CRediT authorship contribution statement

Erika von Schneidemesser: Conceptualization, Methodology, Formal analysis, Writing – original draft, Visualization, Supervision. **Bheki Sibiya:** Formal analysis, Data curation, Visualization, Writing – review & editing. **Alexandre Caseiro:** Methodology, Validation, Formal analysis, Data curation, Writing – review & editing, Visualization. **Tim Butler:** Conceptualization, Methodology, Writing – review & editing. **Mark G. Lawrence:** Conceptualization, Writing – review & editing. **Joana Leitao:** Formal analysis, Data curation, Writing – review & editing. **Aurelia Lupascu:** Methodology, Validation, Formal analysis, Data curation, Visualization, Writing – review & editing. **Pedro Salvador:** Methodology, Formal analysis, Data curation, Writing – review & editing.

Declaration of competing interest

The authors declare that they have no known competing financial interests or personal relationships that could have appeared to influence the work reported in this paper.

Acknowledgements

The authors would like to thank Dr. Andreas Kerschbaumer and the Berlin Senate Department for Environment, Transport and Climate Protection generally for the provision of air quality and traffic count data. The financial support for the IASS Potsdam is provided by the Federal Ministry of Education and Research of Germany (BMBF) and the Ministry for Science, Research and Culture of the State of Brandenburg (MWFK).

Appendix A. Supplementary data

Supplementary data to this article can be found online at https://doi.org/10.1016/j.aeaoa.2021.100122.

CRediT author statement

EvS conceptualization, methodology, formal analysis, writing – original draft, visualization, supervision, BS formal analysis, data curation, visualization, writing – review and editing, AC methodology, validation, formal analysis, data curation, writing – review and editing, visualization, TB conceptualization, methodology, writing – review and editing, MGL conceptualization, writing – review and editing, JL formal analysis, data curation, writing – review and editing, AL methodology, validation, formal analysis, data curation, visualization, writing – review and editing, PS methodology, formal analysis, data curation, writing – review and editing.

References

Barré, J., Petetin, H., Colette, A., Guevara, M., Peuch, V.H., Rouil, L., Engelen, R., Inness, A., Flemming, J., Pérez García-Pando, C., Bowdalo, D., Meleux, F., Geels, C., Christensen, J.H., Gauss, M., Benedictow, A., Tsyro, S., Friese, E., Struzewska, J., Kaminski, J.W., Douros, J., Timmermans, R., Robertson, L., Adani, M., Jorba, O., Joly, M., Kouznetsov, R., 2020. Estimating lockdown induced European NO2 changes. Atmos. Chem. Phys. Discuss. 2020, 1–28.

Belis, C., Favez, O., Mircea, M., Diapouli, E., Manousakas, M., Vratolis, S., Gilardoni, S., Paglione, M., Decesari, S., Mocnik, G., Mooibroek, D., Salvador, P., Takahama, S., Vecchi, R., Paatero, P., 2019. European Guide on Air Pollution Source Apportionment with Receptor Models, Luxembourg.

Blanchard, C.L., Tanenbaum, S., Lawson, D.R., 2008. Differences between weekday and weekend air pollutant levels in Atlanta; Baltimore; Chicago; Dallas–Fort worth; Denver; Houston; New York; Phoenix; Washington, DC; and surrounding areas. J. Air Waste Manag. Assoc. 58, 1598–1615.

BMVI, 2018. Mobilität in Deutschland: Ergebnisbericht. Bundesministerium für Verkehr und digitale Infrastruktur, Bonn, Germany.

Briz-Redón, Á., Belenguer-Sapiña, C., Serrano-Aroca, Á., 2021. Changes in air pollution during COVID-19 lockdown in Spain: a multi-city study. J. Environ. Sci. (China) 101, 16–26.

Burnett, R., Chen, H., Szyszkowicz, M., Fann, N., Hubbell, B., Pope, C.A., Apte, J.S., Brauer, M., Cohen, A., Weichenthal, S., Coggins, J., Di, Q., Brunekreef, B., Frostad, J., Lim, S.S., Kan, H., Walker, K.D., Thurston, G.D., Hayes, R.B., Lim, C.C., Turner, M.C., Jerrett, M., Krewski, D., Gapstur, S.M., Diver, W.R., Ostro, B., Goldberg, D., Crouse, D.L., Martin, R.V., Peters, P., Pinault, L., Tjepkema, M., van Donkelaar, A., Villeneuve, P.J., Miller, A.B., Yin, P., Zhou, M., Wang, L., Janssen, N. A.H., Marra, M., Atkinson, R.W., Tsang, H., Quoc Thach, T., Cannon, J.B., Allen, R. T., Hart, J.E., Laden, F., Cesaroni, G., Forastiere, F., Weinmayr, G., Jaensch, A., Nagel, G., Concin, H., Spadaro, J.V., 2018. Global estimates of mortality associated with long-term exposure to outdoor fine particulate matter. Proc. Natl. Acad. Sci. Unit. States Am. 115, 9592.

Butler, T., Lupascu, A., Nalam, A., 2020. Attribution of ground-level ozone to anthropogenic and natural sources of nitrogen oxides and reactive carbon in a global chemical transport model. Atmos. Chem. Phys. 20, 10707–10731.

Chin, M., Ginoux, P., Kinne, S., Torres, O., Holben, B.N., Duncan, B.N., Martin, R.V., Logan, J.A., Higurashi, A., Nakajima, T., 2002. Tropospheric aerosol optical thickness from the GOCART model and comparisons with satellite and sun photometer measurements. J. Atmos. Sci. 59, 461–483.

Cohen, A.J., Brauer, M., Burnett, R., Anderson, H.R., Frostad, J., Estep, K., Balakrishnan, K., Brunekreef, B., Dandona, L., Dandona, R., Feigin, V., Freedman, G., Hubbell, B., Jobling, A., Kan, H., Knibbs, L., Liu, Y., Martin, R., Morawska, L., Pope, C.A., Shin, H., Straif, K., Shaddick, G., Thomas, M., van Dingenen, R., van Donkelaar, A., Vos, T., Murray, C.J.L., Forouzanfar, M.H., 2017. Estimates and 25-year trends of the global burden of disease attributable to ambient air pollution: an analysis of data from the Global Burden of Diseases Study 2015. Lancet 389, 1907–1918.

Cole, M.A., Ozgen, C., Strobl, E., 2020. Air pollution exposure and Covid-19 in Dutch municipalities. Environ. Resour. Econ. 76, 581–610.

Copat, C., Cristaldi, A., Fiore, M., Grasso, A., Zuccarello, P., Signorelli, S.S., Conti, G.O., Ferrante, M., 2020. The role of air pollution (PM and NO2) in COVID-19 spread and lethality: a systematic review. Environ. Res. 191.

Creutzig, F., Javaid, A., Soomauroo, Z., Lohrey, S., Milojevic-Dupont, N., Ramakrishnan, A., Sethi, M., Liu, L., Niamir, L., Bren d'Amour, C., Weddige, U., Lenzi, D., Kowarsch, M., Arndt, L., Baumann, L., Betzien, J., Fonkwa, L., Huber, B., Mendez, E., Misiou, A., Pearce, C., Radman, P., Skaloud, P., Zausch, J.M., 2020. Fair street space allocation: ethical principles and empirical insights. Transport Rev. 40, 711–733.

Dudhia, J., 1989. Numerical study of convection observed during the winter monsoon experiment using a mesoscale two-dimensional model. J. Atmos. Sci. 46, 3077–3107.

EC, 2015. Directive 2008/50/EC of the European Parliament and of the Council of 21 May 2008 on Ambient Air Quality and Cleaner Air for Europe, in: Union, E. (Ed.), Directive 2008/50/EC.

EEA, 2019. Exceedances of Air Quality Limit Values Due to Traffic. European Environment Agency.

EEA, 2020. Exceedance of Air Quality Standards in Europe. European Environment Agency.

Fast, J.D., Gustafson Jr., W.I., Easter, R.C., Zaveri, R.A., Barnard, J.C., Chapman, E.G., Grell, G.A., Peckham, S.E., 2006. Evolution of ozone, particulates, and aerosol direct radiative forcing in the vicinity of Houston using a fully coupled meteorology-chemistry-aerosol model. J. Geophys. Res.: Atmos. 111.

Gama, C., Relvas, H., Lopes, M., Monteiro, A., 2021. The impact of COVID-19 on air quality levels in Portugal: a way to assess traffic contribution. Environ. Res. 193, 110515.

Gerike, R., Hubrich, S., Ließke, F., Wittig, S., Wittwer, R., 2019. Mobilität in Städten 2018: Mobilitätssteckbrief für Berlin. TU Dresden, Dresden, Germany.

Goldberg, D.L., Anenberg, S.C., Griffin, D., McLinden, C.A., Lu, Z., Streets, D.G., 2020. Disentangling the impact of the COVID-19 lockdowns on urban NO2 from natural variability. Geophys. Res. Lett. 47, e2020GL089269.

Grange, S.K., Lee, J.D., Drysdale, W.S., Lewis, A.C., Hueglin, C., Emmenegger, L., Carslaw, D.C., 2020. COVID-19 lockdowns highlight a risk of increasing ozone pollution in European urban areas. Atmos. Chem. Phys. Discuss. 2020, 1–25.

Grell, G.A., Peckham, S.E., Schmitz, R., McKeen, S.A., Frost, G., Skamarock, W.C., Eder, B., 2005. Fully coupled "online" chemistry within the WRF model. Atmos. Environ. 39, 6957–6975.

Guenther, A., Karl, T., Harley, P., Wiedinmyer, C., Palmer, P.I., Geron, C., 2006. Estimates of global terrestrial isoprene emissions using MEGAN (model of emissions of gases and aerosols from nature). Atmos. Chem. Phys. 6, 3181–3210.

Guevara, M., Jorba, O., Soret, A., Petetin, H., Bowdalo, D., Serradell, K., Tena, C., Denier van der Gon, H., Kuenen, J., Peuch, V.H., Pérez García-Pando, C., 2020. Time-resolved emission reductions for atmospheric chemistry modelling in Europe during the COVID-19 lockdowns. Atmos. Chem. Phys. Discuss. 2020, 1–37.

Hong, S.-Y., Noh, Y., Dudhia, J., 2006. A new vertical diffusion package with an explicit treatment of entrainment processes. Mon. Weather Rev. 134, 2318–2341.

Huth, R., Beck, C., Philipp, A., Demuzere, M., Ustrnul, Z., Cahynová, M., Kyselý, J., Tveito, O.E., 2008. Classifications of atmospheric circulation patterns. Ann. N. Y. Acad. Sci. 1146, 105–152.

Jimenez, P.A., Dudhia, J., González-Rouco, J.F., Navarro, J., Montávez, J.P., García-Bustamante, E., 2012. A revised scheme for the WRF surface layer formulation. Mon. Weather Rev. 140, 898–918.

Jonson, J.E., Schulz, M., Emmons, L., Flemming, J., Henze, D., Sudo, K., Tronstad Lund, M., Lin, M., Benedictow, A., Koffi, B., Dentener, F., Keating, T., Kivi, R., Davila, Y., 2018. The effects of intercontinental emission sources on European air pollution levels. Atmos. Chem. Phys. 18, 13655–13672.

Kain, J.S., 2004. The Kain?Fritsch convective parameterization: an update. J. Appl. Meteorol. 43, 170–181.

Kalnay, E., Kanamitsu, M., Kistler, R., Collins, W., Deaven, D., Gandin, L., Iredell, M., Saha, S., White, G., Woollen, J., Zhu, Y., Chelliah, M., Ebisuzaki, W., Higgins, W., Janowiak, J., Mo, K.C., Ropelewski, C., Wang, J., Leetmaa, A., Reynolds, R., Jenne, R., Joseph, D., 1996. The NCEP/NCAR 40-year Reanalysis project. Bull. Am. Meteorol. Soc. 77, 437–472.

Karl, T., Graus, M., Striednig, M., Lamprecht, C., Hammerle, A., Wohlfahrt, G., Held, A., von der Heyden, L., Deventer, M.J., Krismer, A., Haun, C., Feichter, R., Lee, J., 2017. Urban eddy covariance measurements reveal significant missing NOx emissions in Central Europe. Sci. Rep. 7, 2536.

Kroll, J.H., Heald, C.L., Cappa, C.D., Farmer, D.K., Fry, J.L., Murphy, J.G., Steiner, A.L., 2020. The complex chemical effects of COVID-19 shutdowns on air quality. Nat. Chem. 12, 777–779.

Kuik, F., Lauer, A., Churkina, G., Denier van der Gon, H.A.C., Fenner, D., Mar, K.A., Butler, T.M., 2016. Air quality modelling in the Berlin–Brandenburg region using WRF-Chem v3.7.1: sensitivity to resolution of model grid and input data. Geosci. Model Dev. (GMD) 9, 4339–4363.

Kuik, F., Kerschbaumer, A., Lauer, A., Lupascu, A., von Schneidemesser, E., Butler, T.M., 2018. Top–down quantification of NOx emissions from traffic in an urban area using a high-resolution regional atmospheric chemistry model. Atmos. Chem. Phys. 18, 8203–8225.

Lee, J.D., Helfter, C., Purvis, R.M., Beevers, S.D., Carslaw, D.C., Lewis, A.C., Møller, S.J., Tremper, A., Vaughan, A., Nemitz, E.G., 2015. Measurement of NOx fluxes from a tall tower in central London, UK and comparison with emissions inventories. Environ. Sci. Technol. 49, 1025–1034.

Lelieveld, J., Klingmüller, K., Pozzer, A., Pöschl, U., Fnais, M., Daiber, A., Münzel, T., 2019. Cardiovascular disease burden from ambient air pollution in Europe reassessed using novel hazard ratio functions. Eur. Heart J. 40, 1590–1596.

López-Feldman, A., Heres, D., Marquez-Padilla, F., 2021. Air pollution exposure and COVID-19: a look at mortality in Mexico City using individual-level data. Sci. Total Environ. 756.

Menut, L., Bessagnet, B., Siour, G., Mailler, S., Pennel, R., Cholakian, A., 2020. Impact of lockdown measures to combat Covid-19 on air quality over western Europe. Sci. Total Environ. 741.

Mlawer, E.J., Taubman, S.J., Brown, P.D., Iacono, M.J., Clough, S.A., 1997. Radiative transfer for inhomogeneous atmospheres: RRTM, a validated correlated-k model for the longwave. J. Geophys. Res.: Atmos. 102, 16663–16682.

Morrison, H., Thompson, G., Tatarskii, V., 2009. Impact of cloud microphysics on the development of trailing stratiform precipitation in a simulated squall line: comparison of one- and two-moment schemes. Mon. Weather Rev. 137, 991–1007.

Oikonomakis, E., Aksoyoglu, S., Ciarelli, G., Baltensperger, U., Prévôt, A.S.H., 2018. Low modeled ozone production suggests underestimation of precursor emissions (especially NOx) in Europe. Atmos. Chem. Phys. 18, 2175–2198.

Ordóñez, C., Garrido-Perez, J.M., García-Herrera, R., 2020. Early spring near-surface ozone in Europe during the COVID-19 shutdown: meteorological effects outweigh emission changes. Sci. Total Environ. 747.

Petetin, H., Bowdalo, D., Soret, A., Guevara, M., Jorba, O., Serradell, K., Pérez García-Pando, C., 2020. Meteorology-normalized impact of the COVID-19 lockdown upon NO2 pollution in Spain. Atmos. Chem. Phys. 20, 11119–11141.

Pfister, G.G., Parrish, D.D., Worden, H., Emmons, L.K., Edwards, D.P., Wiedinmyer, C., Diskin, G.S., Huey, G., Oltmans, S.J., Thouret, V., Weinheimer, A., Wisthaler, A., 2011. Characterizing summertime chemical boundary conditions for airmasses entering the US West Coast. Atmos. Chem. Phys. 11, 1769–1790.

Pozzer, A., Dominici, F., Haines, A., Witt, C., Münzel, T., Lelieveld, J., 2020. Regional and global contributions of air pollution to risk of death from COVID-19. Cardiovasc. Res. 116, 2247–2253.

Salvador, P., Artíñano, B., Pio, C., Afonso, J., Legrand, M., Puxbaum, H., Hammer, S., 2010. Evaluation of aerosol sources at European high altitude background sites with trajectory statistical methods. Atmos. Environ. 44, 2316–2329.

Salvador, P., Alonso-Pérez, S., Pey, J., Artíñano, B., de Bustos, J.J., Alastuey, A., Querol, X., 2014. African dust outbreaks over the western Mediterranean Basin: 11-year characterization of atmospheric circulation patterns and dust source areas. Atmos. Chem. Phys. 14, 6759–6775.

Salvador, P., Barreiro, M., Gómez-Moreno, F.J., Alonso-Blanco, E., Artíñano, B., 2021. Synoptic classification of meteorological patterns and their impact on air pollution episodes and new particle formation processes in a south European air basin. Atmos. Environ. 245, 118016.

Sicard, P., Paoletti, E., Agathokleous, E., Araminienė, V., Proietti, C., Coulibaly, F., De Marco, A., 2020a. Ozone weekend effect in cities: deep insights for urban air pollution control. Environ. Res. 191, 110193.

Sicard, P., De Marco, A., Agathokleous, E., Feng, Z., Xu, X., Paoletti, E., Rodriguez, J.J.D., Calatayud, V., 2020b. Amplified ozone pollution in cities during the COVID-19 lockdown. Sci. Total Environ. 735.

Steinbrecht, W., Kubistin, D., Plass-Dülmer, C., Davies, J., Tarasick, D.W., Gathen, P.v.d, Deckelmann, H., Jepsen, N., Kivi, R., Lyall, N., Palm, M., Notholt, J., Kois, B., Oelsner, P., Allaart, M., Piters, A., Gill, M., Van Malderen, R., Delcloo, A.W., Sussmann, R., Mahieu, E., Servais, C., Romanens, G., Stübi, R., Ancellet, G., Godin-Beekmann, S., Yamanouchi, S., Strong, K., Johnson, B., Cullis, P., Petropavlovskikh, I., Hannigan, J.W., Hernandez, J.-L., Diaz Rodriguez, A., Nakano, T., Chouza, F., Leblanc, T., Torres, C., Garcia, O., Röhling, A.N., Schneider, M., Blumenstock, T., Tully, M., Paton-Walsh, C., Jones, N., Querel, R., Strahan, S., Stauffer, R.M., Thompson, A.M., Inness, A., Engelen, R., Chang, K.-L., Cooper, O.R., 2021. COVID-19 crisis reduces free tropospheric ozone across the northern Hemisphere. Geophys. Res. Lett. 48, e2020GL091987.

Travaglio, M., Yu, Y., Popovic, R., Selley, L., Leal, N.S., Martins, L.M., 2021. Links between air pollution and COVID-19 in England. Environ. Pollut. 268.

Valverde, V., Pay, M.T., Baldasano, J.M., 2015. Circulation-type classification derived on a climatic basis to study air quality dynamics over the Iberian Peninsula. Int. J. Climatol. 35, 2877–2897.

Veratti, G., Fabbi, S., Bigi, A., Lupascu, A., Tinarelli, G., Teggi, S., Brusasca, G., Butler, T. M., Ghermandi, G., 2020. Towards the coupling of a chemical transport model with a micro-scale Lagrangian modelling system for evaluation of urban NOx levels in a European hotspot. Atmos. Environ. 223, 117285.